JASS 2008 - Joint Advanced Student School, Saint Petersburg, 9. - 19.3.2008
Modelling and Simulation in Multidisciplinary Engineering

Design and Simulation of a Nano-particle-Reactor

Mangesius H.
Technische Universität München,
Lehrstuhl für Fluidmechanik – Fachgebiet Gasdynamik,
D-85747 Garching Germany

Content

1 Introduction
1.1 Analytical Tools and Simulation
1.2 Technology of Nano-particles
2 The Nano-particle-Reactor
2.1 Overview and Multidisciplinary Set of Problem
2.2 Design with Simplified Models
2.3 2-D Inviscid Simulations
2.4 Decomposition and Particle Growth
2.5 Gasdynamic Quenching
3 Conclusion

Abstract

The focus of this paper is the application of analytical and numerical tools on the gasdynamically induced nano-particles. A new method for synthesizing nano-particles from the gas-phase in a transonic reactor is depicted. The importance of analytical tools for efficient numerical simulations and the preliminary design process is shown. In order to simulate the particle dynamics a monodisperse, bimodal particle model is coupled with the flow simulation. Finally a single phase simulation of the gasdynamic concept is presented.

1 Introduction

Engineering and scientific work together with technical advances lead to a high degree of multidisciplinarity. In emerging technologies the adoption of numerical tools and simulation increases.

1.1 Analytical Tools and Simulation

Developments in computation and science within the last decades lead to the demand on new skills and requirements concerning engineering work. Whereas in the past the experiment was dominating in research departments as the way to ensure and validate model and theory, today the numerical simulation adds to this function. Especially for engineering and design purposes the numerical simulation states a powerful tool as it is a cheap and fast process with the advantage of easily realizing many iterations and changing conditions. In this context we always face a risk of confidence and need a validation of results. Therefore, estimations using analytical tools help to ensure the quality of results and to prevent 'try-and-error-infinity-loops' and enable efficient simulation.

1.2 Technology of Nano-particles

The term nano-particle is derived from its dimension which typically lies in the range of 1 to 100 nm. Nano-particles already found their way into many industrial fields and products of our daily lives. In many cases nano-particles are used to enhance the properties of materials for example to enhance elasticity, to provide electrical

conductivity (e.g. transparent conducting oxides in touchscreens), or to enable local processes like 'glue at command' (nanoferrit ensures fast and effective glue curing after activation through microwaves) and chemical reactions through acting as a catalyst carrier. Moreover, nano-particles play an important role in life science. The adoption ranges from effective sun protection (TiO_2 as UV-filter), self-cleaning surfaces, electronics (e.g. SiO_2 for polishing wafer) to nano-particles in medicine as drug delivery system, in antibacterial coatings or in tumour therapy (hypothermia with magnetic nanoferrits) and in cosmetics through enabling new colour effects and an optical reduction of wrinkles.

The high applicable potential leads to a rise in synthesizing and adoption of a high variety of nano-particles. Today synthesizing nano-particles is carried out in chemical as well as in mechanical processes, in processes using lithography, plasma or flame heating, self-organized growth on surfaces or nucleation of molecules from a gasphase (aerosol processes). Usually industries demand a defined and narrow particle-size distribution. Synthesizing processes which fulfil this condition are currently not applicable for a large-scale production of nano-particles.

The new process of 'gasdynamical induced nano-particles' [1] promises to close this gap. A narrow particle size distribution is ensured by heating and cooling rates in the scale of 10^7 K/s using aerodynamic quenching and heating across a shock.

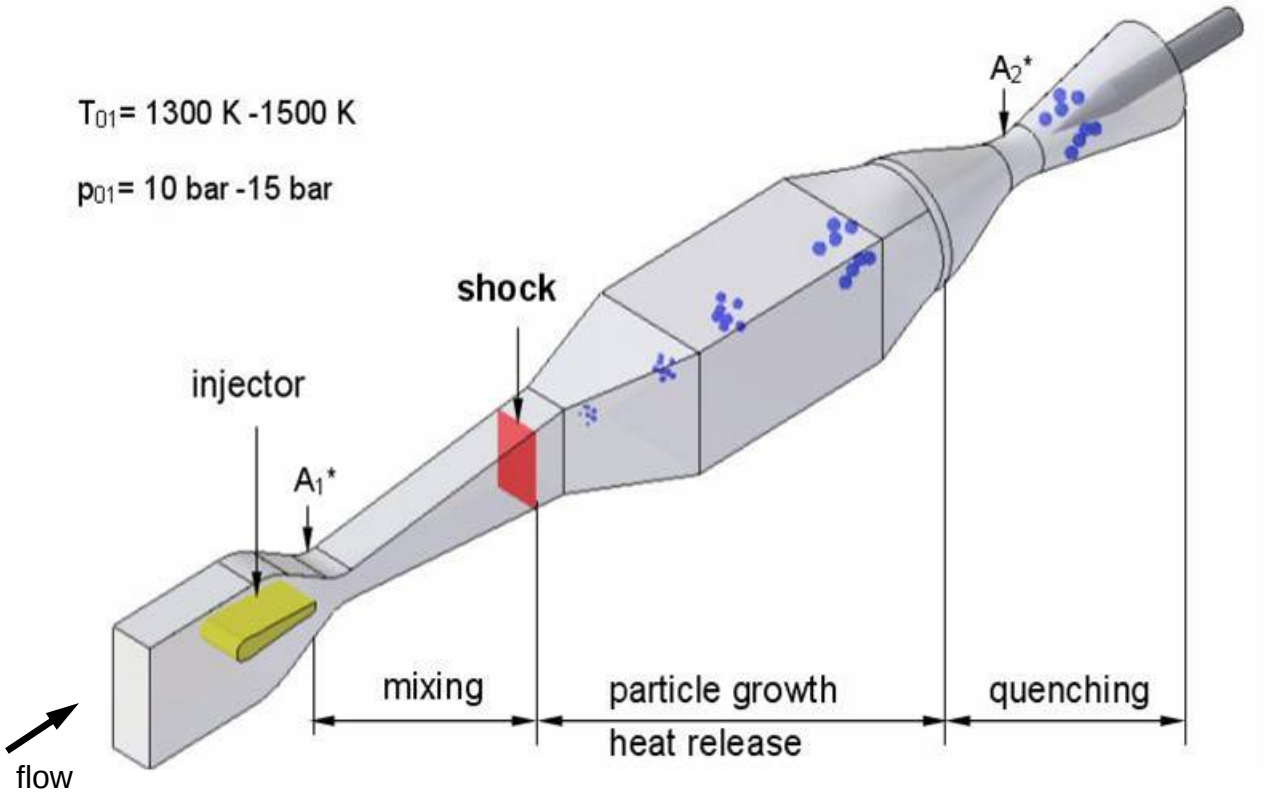

Figure 1: Sketch of the nano-particle reactor

In contrast to standard large-scale synthesizing processes a homogeneous flow field is obtained and thermodynamic conditions stating the parameter of the reaction and the particle growth can be controlled [2]. Inter alia the homogeneous particle size is based on a fast under-run of the saturation limit. Therefore, no nucleation takes part and all monomers are of the size of a siliciumdioxid molecule. The degree of saturation S is calculated by the fraction of the partial pressure of condensable components p_v and the saturation pressure of vaporous components $p_S(T)$ [3].

$$S = \frac{p_v}{p_S(T)}. \qquad (1)$$

Due to a value of about 1000 for S a homogenous nuclei size is obtained. The research project 'gasdynamically induced nano-particles' is supported by the DFG (Deutsche Forschungsgemeinschaft). It is promoted by industrial partners, university partners as well as research institutes. The technology is already worldwide patent-registered.

2 The Nano-particle-Reactor

The principle of the production of oxide nano-particles from gas-phase precursors in a transonic reactor is depicted in Fig. 2. Comprehensive simulations in combination with analytical calculations and comparison with experiments are used to investigate the underlying fluid-dynamic and chemical-kinetic requirements to compose a design strategy of a pilot facility [1].

2.1 Overview and Multidisciplinary Set of Problem

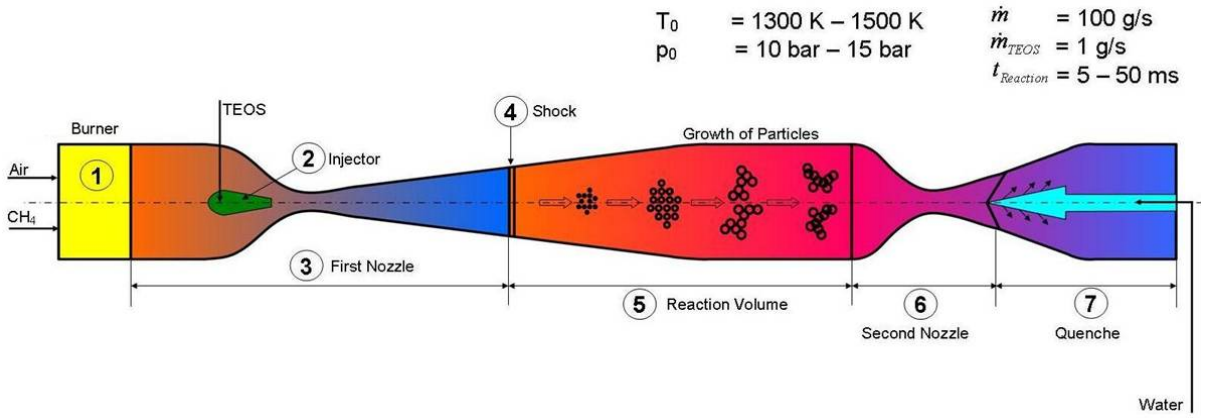

Figure 2: Principle of operation of the nano-particle reactor

The total temperature of the gas is provided by a burner (1). After the injection of the precursor gas (2) the flow accelerates to supersonic flow speed in the first nozzle (3) and the reaction is initiated by shock heating (4). Chemical processes lead to the generation and growth of nano-particles in the reaction chamber (5). After an adjustable reaction time depending on the gas velocity and the reactor length, the reaction is terminated due to rapid expansion and, therefore, cooling of the gas in a convergent-divergent nozzle flow (6) in which the flow again is accelerated to supersonic flow speed. The total enthalpy of the flow is reduced by injecting water in a quenching system downstream of the second nozzle throat (7) [1].

The improtant elements in this multidisciplinary set of problem are the two Laval nozzles with a double choked flow, flow with heat addition and a reaction and particle model that has to be coupled with the flow simulation.

2.2 Design with Simplified Models

The basic layout of the first nozzle is defined by the pre-shock Mach number and the design mass flow rate. Essential for implementing a model and starting a numerical simulation of the reactor is the throat area of the second nozzle that has to be matched according to the change of the critical density and total temperature as a result of the shock losses, the viscous losses, the reactive heat addition and wall cooling. A straight forward analytical approach is needed to obtain the value of the second nozzle throat area. Therefore the 1-D analogous model in Fig. 3 is used.

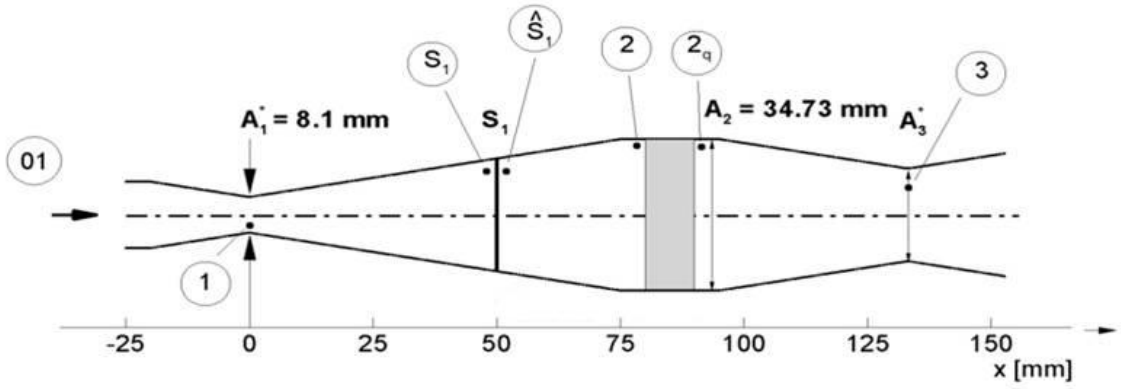

Figure 3: 1-D analogous model, inviscid, heat addition

The given values for the calculation of the area A_3^* in Fig. 3 are the total temperature T_{01}, the total pressure p_{01}, the throat area of the first nozzle A_1^* the cross sectional area A_2 and the heat addition $Q = \frac{q}{c_p \cdot T_{01}}$ as well as the pre-shock Mach number M_{S1}.

Considering conservation of mass

$$\dot{m} = \rho \cdot w \cdot A = \rho_1 * \cdot w_1 * \cdot A_1 * = \rho_3 * \cdot w_3 * \cdot A_3 * \tag{2}$$

and the isentropic relations against the Mach number

$$p_0 = p * \left(\frac{\kappa + 1}{2} \right)^{\frac{\kappa}{\kappa - 1}} \tag{3}$$

$$T_0 = T * \left(\frac{\kappa + 1}{2} \right) \tag{4}$$

as well as the ideal gas law and the relation for sonic speed in ideal gas

$$\rho * = \frac{p *}{R\, T *} \tag{5}$$

$$w^* = c^* = \sqrt{\kappa\, R\, T^*} \tag{6}$$

the mass flow through the reactor can be derived as

$$\dot{m} = \rho^* \cdot w^* \cdot A^* = \frac{p_0 \cdot A^*}{\sqrt{T_0}} \cdot \sqrt{\frac{\kappa}{R}\left(\frac{2}{\kappa+1}\right)^{\frac{\kappa+1}{\kappa-1}}} = const. \tag{7}$$

Here we consider the critical values marked with '*'. In equation 7 the mass flow is composed of a term that varies in pressure and temperature with given sectional area and a constant term. Comparing the mass flow formulation 7 at position (1) and (3) in Fig. 3 (with $\kappa = const.$) leads to the relation of throat areas in the second and first nozzle

$$\frac{A_3^*}{A_1^*} = \frac{p_{01} \cdot \sqrt{T_{03}}}{p_{03} \cdot \sqrt{T_{01}}}. \tag{8}$$

The additional energy input in figure 3 between position (2) and (2_q) results in a rise of total temperature.

$$T_{03} = (1+Q) \cdot T_{01}. \tag{9}$$

Equation 8 with equation 9 becomes:

$$\frac{A_3^*}{A_1^*} = \frac{p_{01}}{p_{03}} \cdot \sqrt{(1+Q)} \tag{10}$$

As Q is know the wanted value of A_3^* just depends on the relation of total pressures considered at the respective positions. Therefore, the changes of total pressure across the shock 11 and across the heat addition 12 have to be calculated in order to obtain p_{03} [4].

$$\frac{\hat{p}_{0\hat{S}_1}}{p_{01}} = \left[1+\frac{2\,\kappa}{\kappa+1}\left(M_{S_1}{}^2-1\right)\right]^{-\frac{1}{\kappa-1}} \cdot \left[1-\frac{2}{\kappa+1}\left(1-\frac{1}{M_{S_1}{}^2}\right)\right]^{-\frac{\kappa}{\kappa-1}} \tag{11}$$

$$\frac{p_{02_q}}{p_{02}} = \frac{M_2{}^2\left(1+\frac{\kappa-1}{2}\,\frac{\kappa+\frac{1}{M_2{}^2}+\sqrt{D}}{\kappa+\frac{1}{M_2{}^2}-\kappa\sqrt{D}}\right)^{\frac{\kappa}{\kappa-1}}\left(\kappa+\frac{1}{M_2{}^2}-\kappa\sqrt{D}\right)}{(\kappa+1)\left(1+\frac{\kappa-1}{2}M_2{}^2\right)^{\frac{\kappa}{\kappa-1}}} \tag{12}$$

with

$$D = \left(\kappa + \frac{1}{M_2^{\,2}}\right)^2 - 2\left(\kappa + 1\right)\left(\frac{1}{M_2^{\,2}} + \frac{\kappa - 1}{2}\right)\left(1 + Q\right). \tag{13}$$

The total pressure at the second nozzle throat equals the total pressure after the heat addition

$$p_{03} = p_{02} \tag{14}$$

Finally the wanted throat area results in

$$A_3^* = A_1^* \cdot \frac{p_{01}}{p_{03}} \cdot \sqrt{\left(1 + Q\right)}\,. \tag{15}$$

The analytical preliminary design geometry for the reactor can be implemented and CFD simulations pursued.

2.3 2-D Inviscid Simulations

In the first case simulations without heat addition are considered in order to understand the flow and its thermodynamic properties. Figure 4 shows the ideal thermo - and fluiddynamic process in the nano-particle-reactor: The flow accelerates in the first nozzle, reaches sonic speed in the throat area and respectively supersonic speed upstream in the divergent nozzle part. Concurrently the static temperature and static pressure are decreasing. As a consequence of the stationary shock the static temperature 'jumps' up to about 500 K. In the second nozzle the flow accelerates from subsonic speed to supersonic speed. Hence, the static temperature decreases fast and aerodynamic quenching is enabled. Considering heat addition one can find the flow speed distribution shown in Fig. 5. Heat addition results in a loss of total pressure concurrently having a choked system due to the supersonic flow speed boundary condition in both nozzles. Respectively the shock position adapts itself to an upstream position with a lower Mach-number leading to a smaller total pressure loss.

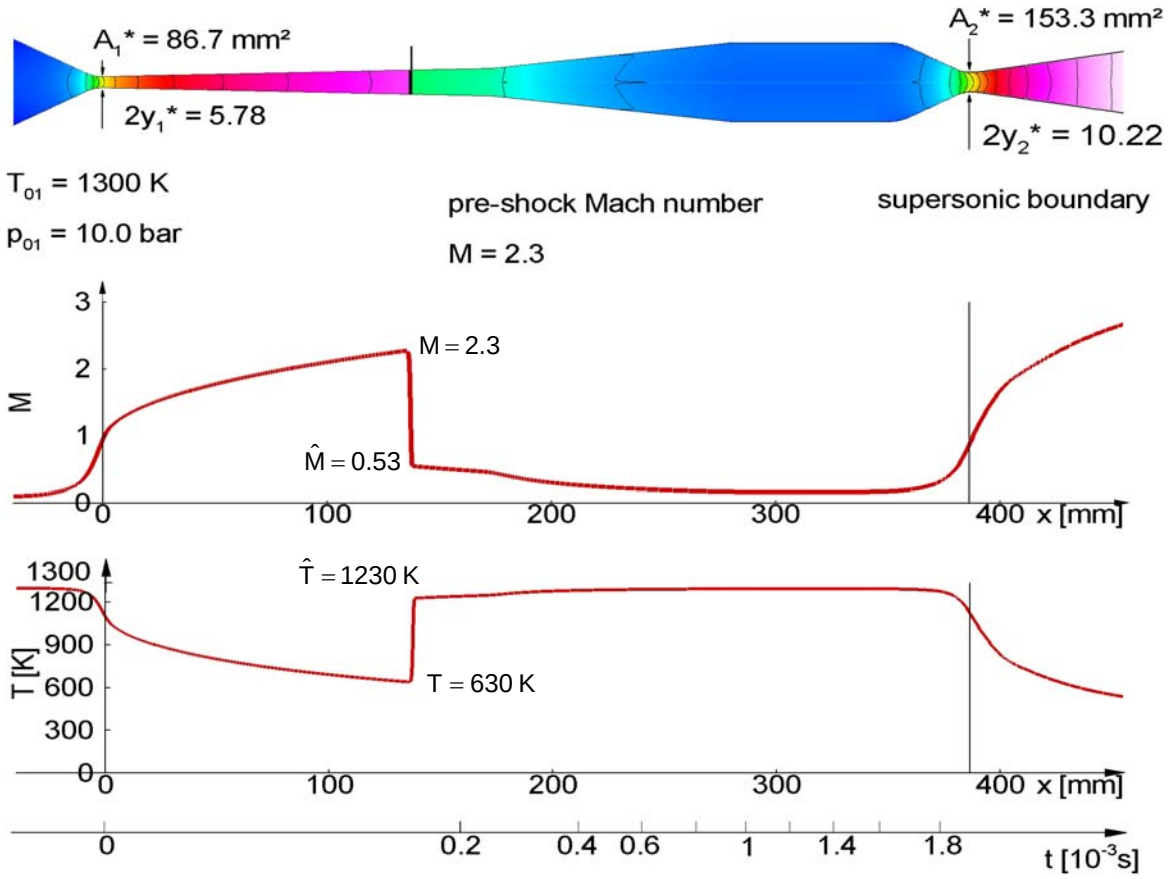

Figure 4: Euler-case, adiabatic

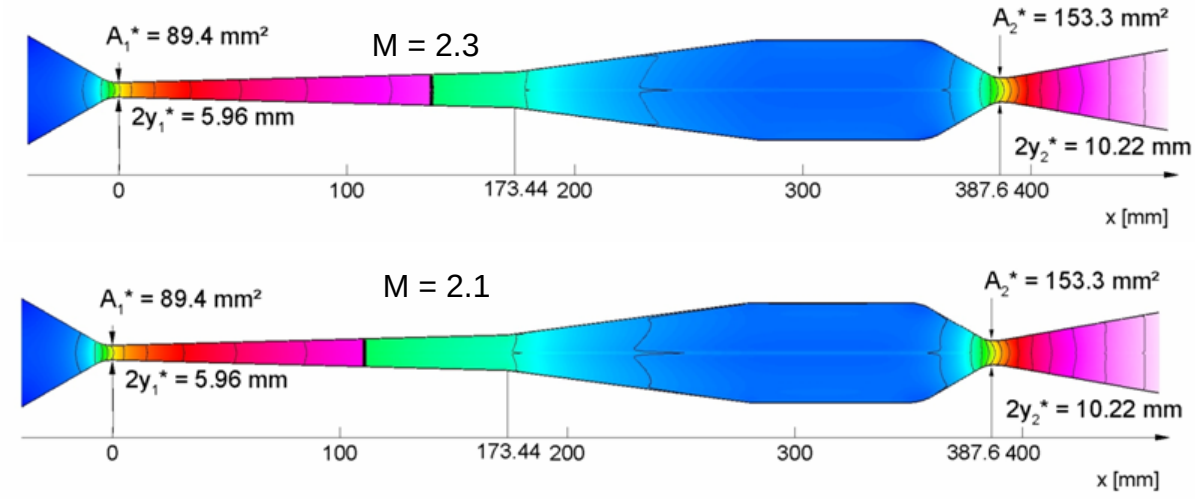

Figure 5: Flow without heat addition (top), flow with heat addition (bottom)

2.4 Decomposition and Particle Growth

The precursor Tetraethoxysilan (TEOS: $Si(OC_2H_5)_4$) is injected into the gas flow at a temperature of 1200 K which is below the ignition limit. The ignition delay τ_{1200K} is $433 \cdot 10^{-3} s$ [1]. The enthalpy of the combustion reaction is 25.4 $\frac{MJ}{kg_{TEOS}}$ with a mass fraction of 1 % of the whole mass flow. Figure 6 shows the processes in the nano-particle reactor: The precursor is injected to the subsonic region ahead of the throat of the first convergent-divergent Laval nozzle. Based on the large velocity difference between the hot gas flow and the injected precursor flow a strong shear stress is generated enhancing the mixing process. After a mixing length and the ignition delay the decomposition and the particle growth process starts. Meanwhile heat is released and monomers start growing to particles. The particle growth is stopped by gasdynamical quenching and instantaneous cooling of the gas-particle mixture.

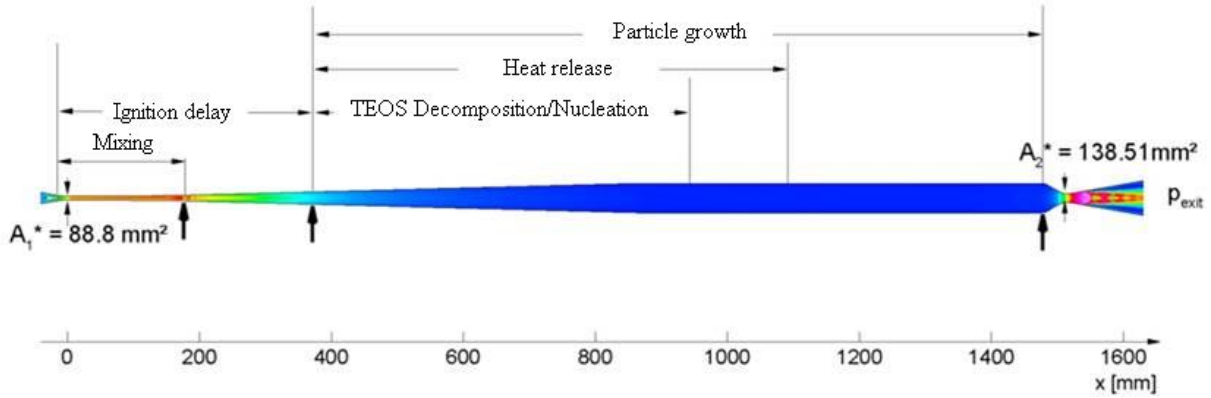

Figure 6: Nano-particle-reactor and reaction/particle-evolution

Due to the large velocity difference at the TEOS injector and the flow pattern downstream the injector the precursor mixes with the surrounding hot gas in vortices (vortex shedding). Figure 7 shows that after a mixing length of 40 mm the mass fraction of TEOS gets close to the global mass fraction of 1 %. Considering the fact that the whole mixing length in the nano-particle reactor is 150 mm a sufficient mixture can be assumed.

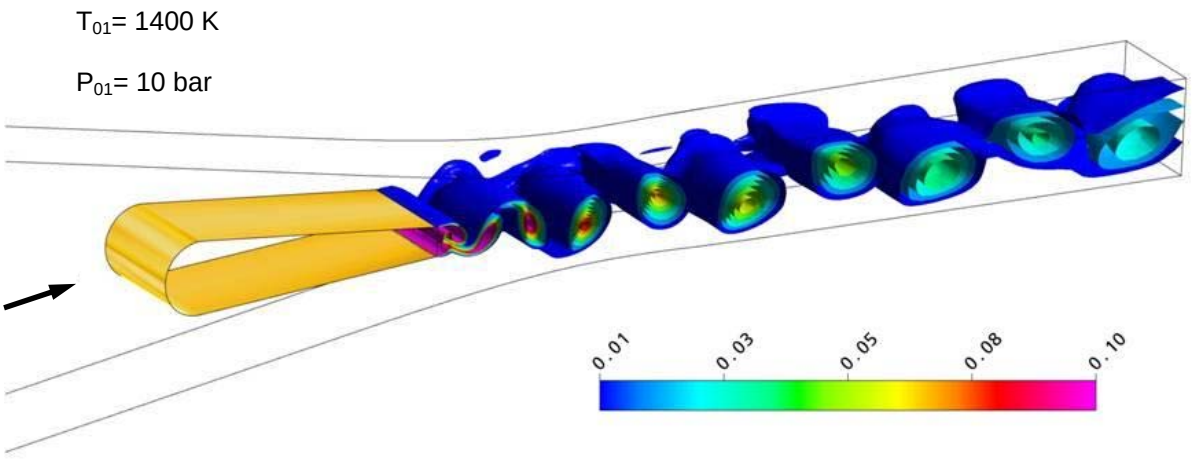

Figure 7: Vortex-shedding and mixture of TEOS with iso-surfaces of the mass fraction

The reaction and particle dynamics are modelled by three partial reactions depicted in Fig 8. The primary reaction is decomposition of the precursor and the production of monomers. It is modelled by a one step reaction described by an Arrhenius equation. The secondary reaction is the formation of critical nuclei. Because of the high supersaturation ratio of the order of 10^3 instantaneously after the primary reaction, the monomers are in our case already critical nuclei and the secondary reaction, the formation of critical nuclei is negligible. The tertiary reaction is the particle growth due to coalescence and coagulation.

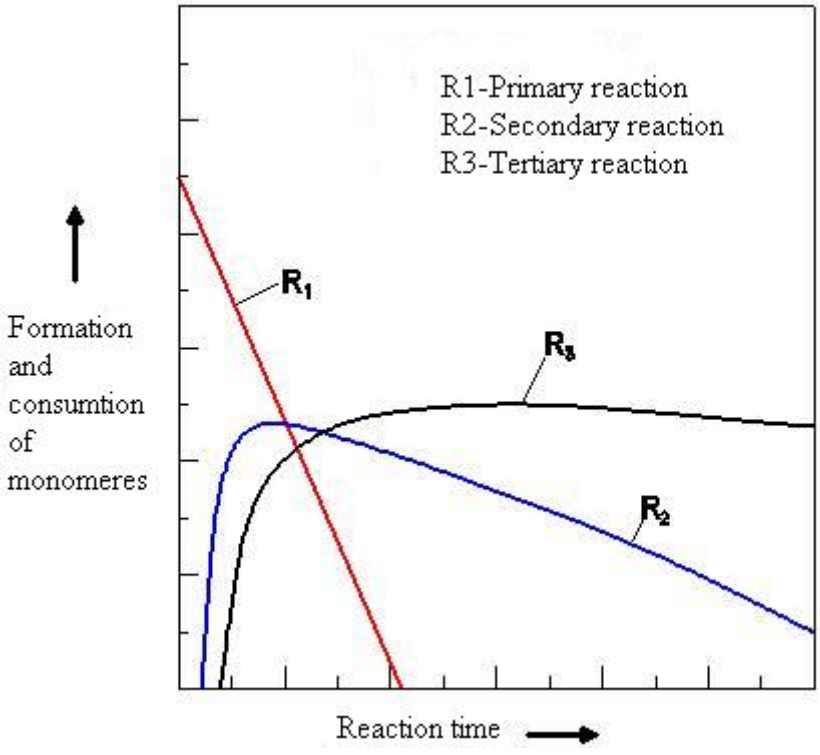

Figure 8: Partial reactions

In this model two discrete monodisperse modes are used to represent the particle size distributions approximately: a size-fixed nucleation mode that accounts for the introduction of newly generated monomers and a moving accumulation mode that describes the particle growth, whereas a particle is defined to consist of at least two monomers [5]. For predicting the nano-particle output of the transonic reactor the particle dynamics described by the monodisperse, bimodal particle model has to be coupled with the Navier Stokes equations. The differential equations describing the TEOS decomposition [6] through the combustion reaction and the heat release are:

$$\dot{n}_{TEOS} = -n_{TEOS} \cdot k_1 \left[\frac{1}{kg \cdot s} \right] \tag{16}$$

with

$$k_1 = 6.7 \cdot 10^{16} \cdot exp\left(\frac{38970K}{T} \right) \frac{1}{s} \tag{17}$$

and

$$\dot{q} = n_B \cdot \frac{1}{N_A} \cdot M_{TEOS} \cdot k_2 \cdot \Delta h_r \left[\frac{J}{kg \cdot s} \right] \tag{18}$$

with

$$k_2 = 6.7 \cdot 10^{15} \cdot exp\left(\frac{38970K}{T} \right) \frac{1}{s}. \tag{19}$$

The heat release is decoupled from the TEOS decomposition as is takes place on a different time scale. In order to describe the particle evolution the coagulation of siliciumdioxid monomers (eq 20), the coagulation of particles (eq 21) and the overall change of particle volume (eq 22) have to be considered. The index 1 stands of a monomer, the index p for a particle.

$$\frac{d}{dt} n_{SiO_2} = n_{TEOS} \cdot k_1 - \rho \cdot \beta_{1,1} \cdot {n_{SiO_2}}^2 - \rho \cdot \beta_{1,P} \cdot n_{SiO_2} \cdot N \left[\frac{1}{kg \cdot s} \right] \tag{20}$$

$$\frac{d}{dt} N = \rho \cdot \frac{1}{2} \beta_{1,1} \cdot {n_{SiO_2}}^2 - \rho \cdot \beta_{P,P} \frac{1}{2} \cdot N^2 - \rho \cdot \frac{1}{2} \beta_{turb} \cdot N^2 \left[\frac{1}{kg \cdot s} \right] \tag{21}$$

$$\frac{d}{dt} V = \rho \cdot \beta_{1,1} \cdot {n_{SiO_2}}^2 \cdot v_0 + \rho \cdot \beta_{1,P} \cdot n_{SiO_2} \cdot N \cdot v_0 \left[\frac{m^3}{kg \cdot s} \right]. \tag{22}$$

The change of the mass specific number concentration of monomers siliciumdioxid (eq. 20) equals the mass specific number concentration of the decomposed precursor less the coagulated monomers coagulation is modelled between monomer and monomer (index 1,1), monomer and particle (index 1,p) and between particle and particle (index p,p) we consider the . Similar to equation 20 equation 21 can be understood. The particle volume (eq. 22) constantly increases with monomers and particles coagulating.

Figure 9 shows the result of a coupled simulation. The achieved particle size is in the scale of $4 \cdot 10^{-8}$m. The particle growth starts with the ignition. At the length of about 1000 mm the graph becomes steeper as the monomers are disassembled. Hence, only particles, which have a greater volume than monomers, are left for the coagulation process.

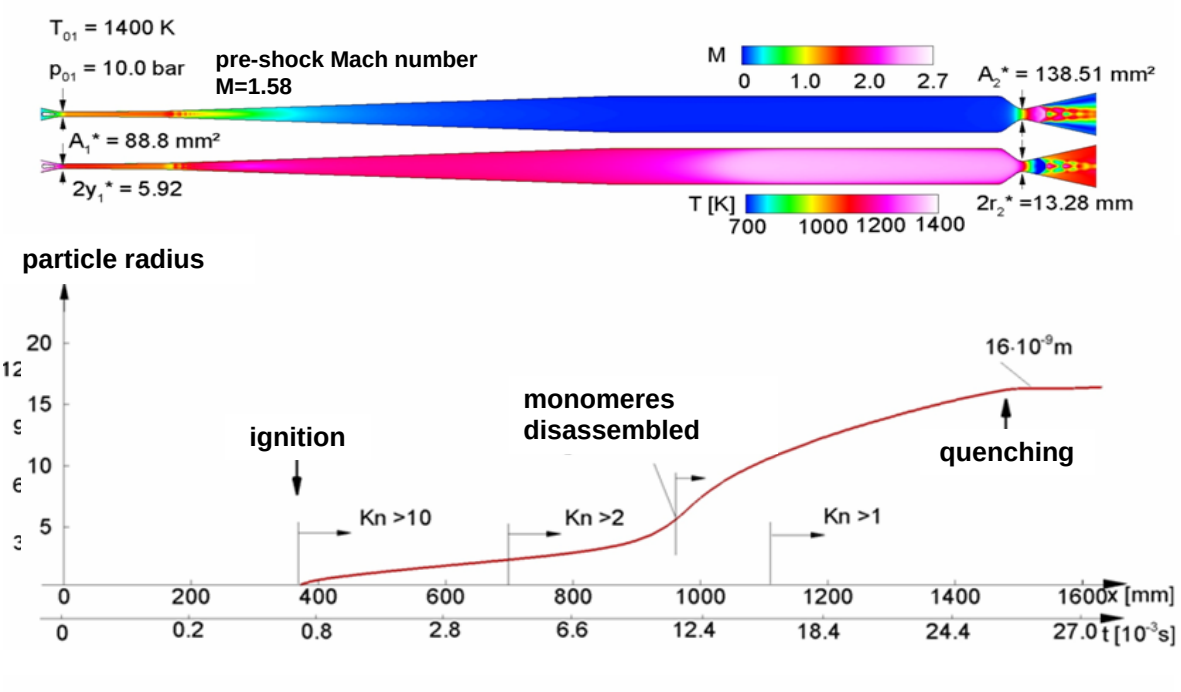

Figure 9: Distribution of particle radius along the axis of the reactor

The particle size distribution in the cross sectional area A shown in Fig. 10 is narrow with a deviation of only 4 nm in the radius.

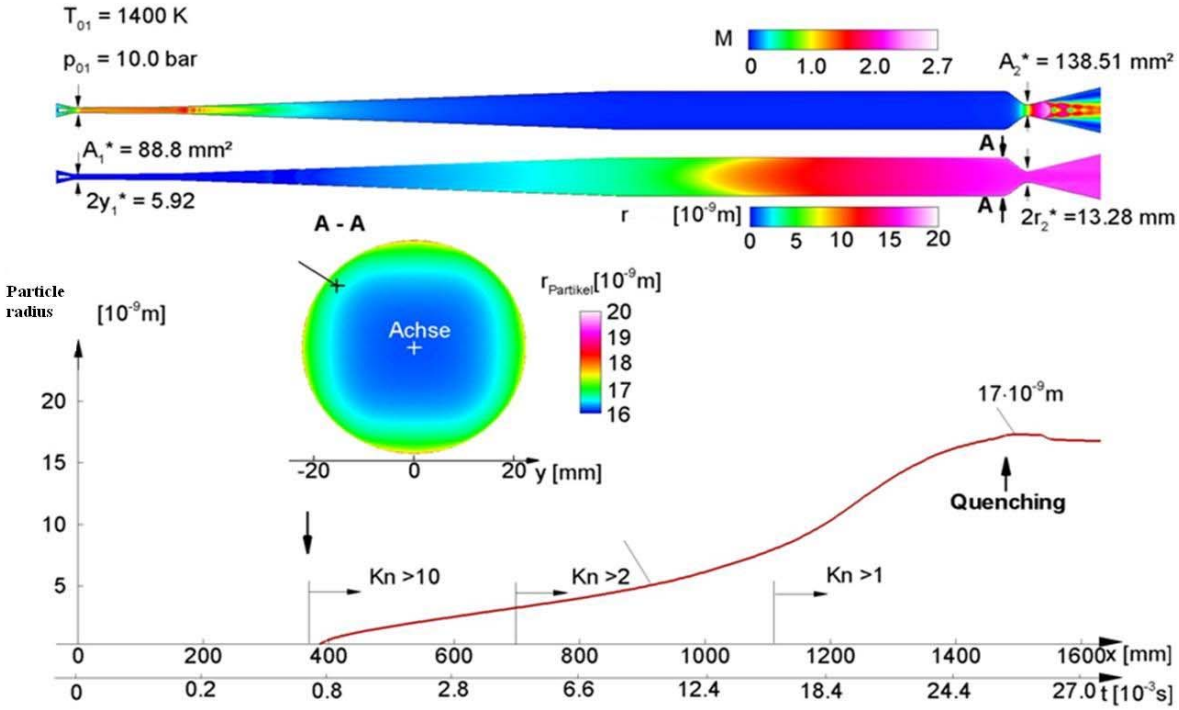

Figure 10: Particle size distribution in a sectional area

3 Conclusion

An analytical and numerical concept for the design of a new reactor for producing nano-particles starting from the gas-phase is presented. Due to the double choked flow in the reactor a straight forward analytical approach is needed in order to enable first geometric reactor modelling. All preliminary simulations are inviscid and 2-dimensional, representing the idea and the ideal case of a shock-wave reactor. The preliminary design of the reactor is carried out through numerical simulations which also contain a particle model.

References

[1] Grzona, A. et al., “Gas-phase Synthesis of Non-agglomerated Nanoparticles by fast Gasdynamic heating and Cooling”, ISSW26 2007 - 26th International Symposium on Shock Waves, Göttingen, Germany, (2007)

[2] Al-Hasan, N., Schnerr, G.H., “Aerodynamic optimization of Laval nozzle flow with shocks: Numerical investigation of active/passive shock control via expansion fans”, Proceedings in Applied Mathematics and Mechanics (2008)

[3] Schaber, K., “Gestalten von Nanopartikeln in der Gasphase und Nanomaterialien“, Institut für Technische Thermodynamik und Kältetechnik, Universität Karlsruhe, Germany, (2006)

[4] Schnerr, G.H., Lecture notes on ‘Gasdynamische Strömungen mit Energiezufuhr und Phasenübergängen’, Technische Universität München 2007.

[5] Jeong, J.I., Choi, M., ”A simple bimodal model for the evolution of non-spherical particles undergoing nucleation, cogulation and coalescence”, Journal of Aerosol Sicence, 34, p.965-976, (2003).

[6] Herzler, J., Manion, J. A., Tsang, W.: Single-Pulse Shock Tube Study of the Decompositionof Tetraethoxysilane and Related Compounds, J. Phys. Chem. A 1997, 101, 5500-5508